

## Shear driven films inside cylinders

I. H. Jahn<sup>1</sup>

<sup>1</sup>School of Mechanical and Mining Engineering  
 The University of Queensland, Brisbane, Queensland 4072, Australia

### Abstract

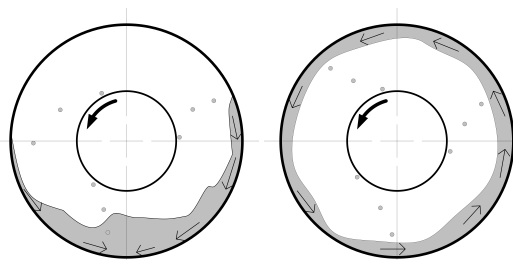
Tangential air shear on the inside of a stationary cylinder, as may exist in the annulus between a concentric rotating and stationary cylinder, can be used to establish a fully wetting film. At low shear a liquid pool is formed at bottom dead center, while at high shear the pool is spread into a film. The development of a thick film model for such conditions is presented. Within the model momentum, gravity, pressure, and wall and air shear are considered to obtain a steady state film solution. Results for a range of operating conditions are presented. Finally by considering the stability of the film solutions as air shear is reduced, the lower limit for film solutions is investigated.

### Introduction

Liquid flow on the inside of cylinders, driven by air shear exist in a number of applications. A specific one is inside high speed gearboxes or bearing chambers, where oil collects on the outer walls. Depending on the geometry and conditions a gravity dominated low shear environment, as shown in Fig. 1(a) may be created. Here the liquid thrown against the walls drains to the bottom. Similarly it is possible to create a high shear environment where the liquid is dominated by air shear as shown in Fig. 1(b). Here the liquid, once on the wall is dominated by air shear and a liquid film moving in the direction of rotation is established.

Chamber operation in both regimes is acceptable, however operation in a transition environment should be avoided as under such conditions highly complex flows can be established, which may lead to undesirable liquid re-entrainment. Consequently tools are required that can predict chamber operation. These tools should be sufficiently simple so that they can be used in the preliminary design phase before the design is frozen.

A key component of the required suite of tools is a liquid film model, which assesses if the air shear in the chamber is sufficient to maintain a liquid film on the wall. This paper describes the first steps in the development of such a model. The current 2-D model aim to model the flow in a circular chamber without any features. Future work will extend the model to incorporate features typically seen in bearing chambers.



(a) Low Shear (b) High Shear

Figure 1: Film flow behaviour

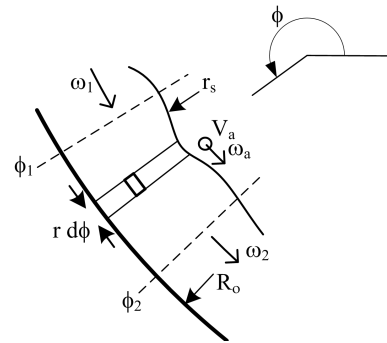


Figure 2: Notation used to describe film

### Model Approach

A number of film models for rimming flow on the inside and outside of cylinders have previously been developed [5, 1]. However they are aimed at very thin films that are approximated using lubrication theory. In chambers and gearboxes, films with a thickness in excess of 1 mm are common [2, 4], resulting in film Reynolds numbers of  $2.0 \times 10^3$  and above. Despite this being close to the transitional Reynolds number, the film is expected to be turbulent, due to the re-circulation vortices described later. Film thicknesses in excess of 5 mm have also been observed by Chandra et al. [2] in the proximity of the sump.

To overcome the limitations of such thin film models, a new model is being developed, based on the momentum balance of the liquid within the film. In such a model the interaction between the liquid and the wall and also between the faster moving air and the film is modelled as representative shear forces. In future, the localised momentum loss introduced by obstacles placed within the film flow can also be incorporated. The challenge of such a model is to correctly define the parameters that govern the momentum exchange. At the moment these parameter are based on literature data, but future work aims to characterise them experimentally. An advantage of this approach is that hydraulic jumps, forming a discontinuity in the film can also be modelled.

### Equations for Liquid Flow

The derivation of the equations governing the film flow in the rotating environment, follows an approach presented by Whitam [6] to analyse flow in open channels. The following derivation, starting from first principles ensures that all rotational effects are correctly accounted for.

By considering the control volume identified in Fig. 2, it can be seen that the conservation of liquid can be expressed as

$$\frac{d}{dt} \int_{\phi_2}^{\phi_1} (R_o^2 - r_s^2) d\phi + [\omega R_o^2 - \omega r_s^2]_{\phi_2}^{\phi_1} + \int_{\phi_2}^{\phi_1} V_a R_o d\phi = 0. \quad (1)$$

The first term is the change of the control volume internal volume, the second is the flux in and out of the control volume at

$\phi_1$  and  $\phi_2$ , and the third the volume addition, where  $V$  is the amount of volume added per unit of circumference.

Analysis of the same control volume yields a conservation equation for angular momentum.

$$\begin{aligned}
& \underbrace{\frac{d}{dt} \int_{\phi_2}^{\phi_1} \frac{1}{2} \omega (R_o^4 - r_s^4) d\phi}_I + \underbrace{\left[ \frac{1}{4} \omega^2 (R_o^4 - r_s^4) \right]}_{II} \\
& + g \sin \phi \underbrace{\left( \frac{1}{2} r_s R_o^2 - \frac{1}{3} R_o^3 - \frac{1}{4} r_s^3 \right)}_{III(a)} + \underbrace{\left[ \frac{1}{8} \omega^2 (R_o^2 - r_s^2)^2 \right]}_{III(b)} \Big|_{\phi_2}^{\phi_1} \\
& = -g \underbrace{\int_{\phi_2}^{\phi_1} \cos \phi \left( \frac{1}{3} R_o^3 - \frac{1}{3} r_s^3 \right) d\phi}_{IV} - \underbrace{\int_{\phi_2}^{\phi_1} \omega_a r_s^2 V_a R_o d\phi}_V \\
& - \underbrace{C_{f,wall} R_o^4 \int_{\phi_2}^{\phi_1} \omega^2 d\phi}_{VI(a)} + \underbrace{C_{f,air} \int_{\phi_2}^{\phi_1} r_s^2 (\omega r_s - \omega_{air} r_s)^2 d\phi}_{VI(b)}. \tag{2}
\end{aligned}$$

The five terms in the equation are, respectively (I) the rate of increase of angular momentum in the section  $\phi_1 < \phi < \phi_2$ , (II) the net angular momentum flux across  $\phi_1$  and  $\phi_2$ , (III) the net total pressure torque acting across  $\phi_1$  and  $\phi_2$ , (IV) the torque created by the tangential component of gravity, (V) the momentum added by the liquid impinging with a speed  $\omega_a$  at the surface, and (VI) the torque created by shear forces. Part (a) corresponds to the wall shear and part (b) to the air shear at the free surface.

The pressure term (III) requires some extra comment. For inviscid flow the radial momentum equation is obtained given from the Euler equation in the radial direction, given by

$$\frac{du_r}{dt} + u_r \frac{du_r}{dr} + \frac{u_\theta}{r} \frac{du_r}{d\phi} - \frac{u_\theta^2}{r} = -\frac{1}{\rho} \frac{dP}{dr} + g_r, \tag{3}$$

where is  $u_r$  and  $u_\theta$  are the velocities in the radial and tangential directions respectively. By neglecting the fluid accelerations in the  $r$  direction, which is permissible as  $u_r \ll u_\theta$  and substituting  $u_\theta = \omega r$  this simplifies to

$$\omega^2 r = -\frac{1}{\rho} \frac{dP}{dr} + g_r, \tag{4}$$

If in accordance with hydraulic theory the angular velocity is averaged out to  $\omega(r, t)$ , Eqn. [4] can be integrated with respect to  $r$ . As  $g_r = g \sin \phi$ , the pressure in the film is given by

$$P - P_0 = \rho \omega^2 \frac{1}{2} (r^2 - r_s^2) - \rho g (r - r_s) \sin \phi. \tag{5}$$

By further integration of Eqn. [5] one obtains term (III) in Eqn. [2]. From the derivation it is evident that part (a) is caused by centrifugal acceleration and part (b) is caused by acceleration due to gravity.

For term (VI) in Eqn. [2], it is assumed that the shear forces at the wall and free surface are given by  $\tau = \rho C_f \Delta v^2$ , where  $\Delta v$  is the velocity difference across the interface.

Equations [1] and [2] are the two conservation equations for  $r_s$  and  $\omega$ . If these two variables are assumed to be continuously differentiable, one can take the limit  $\phi_1 - \phi_2 \rightarrow 0$  to obtain the differential equations for  $r_s$  and  $\omega$ .

$$\frac{d}{dt} (R_o^2 - r_s^2) + \frac{d}{d\phi} (\omega (R_o^2 - r_s^2)) + V_a R_o = 0, \tag{6}$$

$$\begin{aligned}
& \frac{d}{dt} \left( \frac{1}{2} \omega (R_o^4 - r_s^4) \right) + \frac{d}{d\phi} \left[ \frac{1}{4} \omega^2 (R_o^4 - r_s^4) \right] \\
& + g \sin \phi \left( \frac{1}{2} r_s R_o^2 - \frac{1}{3} R_o^3 - \frac{1}{4} r_s^3 \right) + \frac{1}{8} \omega^2 (R_o^2 - r_s^2)^2 \Big|_{\phi_2}^{\phi_1} \\
& = -g \cos \phi \left( \frac{1}{3} R_o^3 - \frac{1}{3} r_s^3 \right) - \omega_a r_s^2 V_a R_o \\
& - C_{f,wall} R_o^4 \omega^2 + C_{f,air} r_s^2 (\omega_{air} r_s - \omega r_s)^2. \tag{7}
\end{aligned}$$

#### Film cavitation criterion

In addition to full-filling the conservation equations [6] and [7], the film is required to remain attached to the outer wall. This criterion is fulfilled as long as the pressure within the film is larger than the surface pressure. By differentiating Eqn. 5 one finds that the radial pressure gradient is given by

$$\frac{dP}{dr} = \rho \omega^2 r - \rho g \sin \phi. \tag{8}$$

This implies the radial pressure gradient is negative for values of  $r$  in the range  $0 < \phi < \pi$  that are below a critical radius given by

$$r_{crit} = \frac{g \sin \phi}{\omega^2}. \tag{9}$$

Hence as long as the film surface radius  $r_s$  is larger than the critical radius the pressure increases inside the film and the film remains attached to the chamber wall. The resulting criterion to avoid film cavitation or detachment is

$$r_s > \frac{g \sin \phi}{\omega^2}. \tag{10}$$

A further implication of the above equations is that with the radially averaged film velocity profile, the first location to see a pressure below gas pressure  $P_0$  is at the film surface. This suggests that if such a solution is approached experimentally, the film starts to fail from the surface, with thin sheets of liquid detaching and falling radially inwards. This effect will be partially counteracted by surface tension, but this effect is currently neglected.

#### Key assumptions

When developing the above equations to analyze the liquid film the key simplification was to average the tangential velocity in the  $r$  coordinate and to neglect accelerations perpendicular to the wall, other than centrifugal.

Normally for shear driven films the velocity profile increases towards the shear driven surface as shown in Fig. 3(a). However a liquid film with such a velocity profile is unstable in a rotating environment. This is the case as the fast moving liquid particles close to the film surface experience a larger centrifugal force than then slower particles at larger radii. The thus created buoyancy like effect caused by differences in centrifugal forces creates secondary re-circulations vortices in the liquid film as shown in Fig. 3(c).

Hence, there is a continuous and significant exchange of momentum between the upper and lower layers, which leads to an averaging of the velocity profile. Consequently, despite the film being driven by surface shear, the tangential velocity profile is likely to resemble the sketch in Fig. 3(b). This means the current approach of radially averaging the tangential velocity is acceptable for steady state solutions.

If studying unsteady effects, further consideration needs to be given to these secondary re-circulations, as accelerations perpendicular to the wall may become significant.

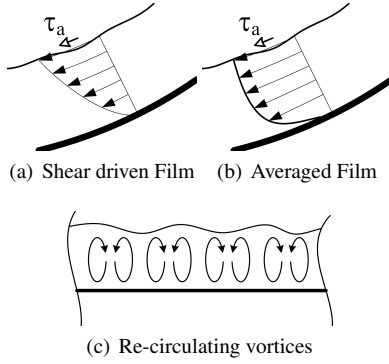


Figure 3: Film velocity profiles and Re-circulation

### Steady State Solution

The steady state solution for the liquid inside the cylinder can be obtained by dropping the time dependant terms from Eqns. [6] and [7]. Under these conditions Eqn. [6] can be integrated to yield

$$\omega (R_o^2 - r_s^2) = \int V(\phi) d\phi + Q_0 = Q(\phi). \quad (11)$$

Here  $Q$  is the volume flow rate in the film, which is the sum of the baseline flow rate  $Q_0$  to which volume is added and subtracted as defined by  $\int V(\phi) d\phi$ . Using Eqn. [11] it is possible to eliminate  $\omega$  from Eqn. [7] to obtain solutions for film height  $r_s(\phi)$  for prescribed film flow rates  $Q(\phi)$  and impinging velocities  $\omega_a(\phi)$ .

For presentation of results, a better comparator is fill fraction  $A_r$ . Fill fraction is defined and calculated using the following formula

$$A_r = \frac{V_L}{V_T} = \left(1 - \frac{1}{2R_o^2\pi} \int_0^{2\pi} r_s^2 d\phi\right). \quad (12)$$

Using  $A_r$  films are compared based on the fraction occupied by liquid in the chamber.

### Results

To provide an insight into film flow inside a chamber, the governing equations are solved for a test chamber. The geometry and the physical properties are given in Tab. 1. For the moment these are based on water as the test medium, as water at ambient temperature has similar physical properties as hot lubricants[2] and as tests using water are planned.

The value for  $C_{f, wall}$ , is based on skin friction values typical for flow across smooth metal surfaces. The value for  $C_{f, air}$  is based on the interface shear measured by Cohen et al. [3]. He measured the shear at the air-liquid interface in a rectangular duct. During these tests the film height was between 0.10 in to 0.25 in (2.5 mm to 6.0 mm) and the air flow created waves with an amplitude of 0.01 in to 0.02 in (0.25 mm to 0.5 mm). These magnitudes are similar to the ones measured on a range of chamber test rigs [2] with films in a rotating environment. This suggests the measurements by Cohen et al. [3] are adequate for the current investigation. His measurements also show that above a mean air speeds of approximately  $14 \text{ ft s}^{-1}$  ( $4.2 \text{ m s}^{-1}$ ), the friction factor  $\lambda_0$ , becomes constant in the range 0.04 to 0.06. For the current model a value of  $\lambda_0 = 0.05$  was chosen, which can be converted into  $C_{f, air}$  using the relationship:

$$C_{f, air} = \frac{\rho_{air}}{\rho_{water}} \frac{1}{8} \lambda_0. \quad (13)$$

Using the constants defined in Tab. 1, the steady state version

$R_o$	0.1 m	$g$	$9.81 \text{ m s}^{-2}$
$\rho_{liquid}$	$1000 \text{ kg m}^{-3}$	$\rho_{air}$	$1.2 \text{ kg m}^{-3}$
$C_{f, wall}$	$2.5 \times 10^{-3}$	$C_{f, air}$	$7.5 \times 10^{-6}$

Table 2: Overview of results for constant air speed

Case	A1	A2	A3	A4	A5
$Q$ ( $\text{m}^2 \text{ s}^{-1}$ )	2	3	4	4.2	4.25
$\omega_{air}$ ( $\text{rad s}^{-1}$ )	350	350	350	350	350
$A_r$ %	1.2	1.9	2.6	2.72	2.76
$(R_o - r_s)_{max}$ (mm / °)	0.80 / 55.8	1.4 / 67.5	2.0 / 73.8	2.1 / 74.7	2.2 / 74.7
$(R_o - r_s)_{min}$ (mm / °)	0.47 / 223.2	0.70 / 235.8	0.93 / 243.9	0.97 / 244.8	0.98 / 245.7
$\omega_{min}$ ( $\text{rad s}^{-1}$ )	12.47	10.94	10.03	9.87	9.86

of Eqn. 7 can be solved for different conditions defined by  $\omega_{air}$ ,  $\omega_a$ , and either  $Q(\phi)$  or  $Q_0$  and  $V_a(\phi)$ . For the moment only cases corresponding to  $\omega_a = 0$  and  $V_a = 0$  have been explored. This corresponds to the case when the chamber contains a constant quantity of liquid. Under these conditions the continuity equation simplifies to  $\omega (R_o^2 - r_s^2) = Q$ , where  $Q$  is a constant. Substituting this into Eqn. [2], results into the elimination of term (III(a)). This implies that the pressure contribution due to centrifugal acceleration only influences the film dynamics if liquid is added or removed and  $Q$  varies with  $\phi$ .

For all test cases it can be seen that the liquid film solutions shows a peak film thickness in the region  $\phi = 0^\circ$  to  $90^\circ$ . This is caused by gravity acting against the direction of flow, leading to a reduction in film velocity, which in turn causes a localised increase in film thickness. Similarly as  $\phi = 90^\circ$  is approached, the gravity component acting in the tangential direction reduces and the film starts to accelerate again.

For the constant air velocity test cases (A1 to A5), shown in Fig. 4, the increase in flow rate  $Q$ , causes an increase in fill fraction  $A_r$ , causes an increase in the amplitude and sharpness of the film thickness peak. Furthermore it is evident that the peak moves towards  $\phi = 90^\circ$  as  $Q$  increases. This can be attributed to term (II) in Eqn. 2 becoming more significant. Effectively more angular momentum is carried by the film. However as  $Q$  is increased beyond  $4.25 \text{ m}^2 \text{ s}^{-1}$ , the cavitation criterion set out in Eqn. 10 is violated in the range  $\phi = 75^\circ$  to  $85^\circ$ , as shown by the thick line section corresponding to case A5 in Fig. 4. This means that with the air speed of  $350 \text{ rad/s}$ , the maximum flow rate  $Q$  that can be maintained equals  $4.2 \text{ m}^2 \text{ s}^{-1}$ , which corresponds to a fill fraction of 2.72%. Higher fill fractions result in film detachment, as insufficient film speed is attained.

Figure 5, shows how air speed affects the film height profile. For all cases except B1, the fill fraction is kept at 2.72%. In case B1, at  $300 \text{ rad s}^{-1}$ , the highest fill fraction resulting in an attached

Table 3: Overview of results for constant fill fraction

Case	B1	B2	B3	B4	B5
$Q$ ( $\text{m}^2 \text{ s}^{-1}$ )	1.24	4.2	5.15	6.73	8.16
$\omega_{air}$ ( $\text{rad s}^{-1}$ )	300	350	400	500	600
$A_r$ (%)	0.9	2.72	2.72	2.72	2.72
$(R_o - r_s)_{max}$ (mm / °)	0.67 / 52.2	2.2 / 74.7	1.8 / 72.9	1.6 / 71.1	1.5 / 70.2
$(R_o - r_s)_{min}$ (mm / °)	0.33 / 213.3	0.98 / 245.7	1.1 / 246.6	1.2 / 247.5	1.2 / 248.8
$\omega_{min}$ ( $\text{rad s}^{-1}$ )	9.22	9.87	14.34	21.13	27.06

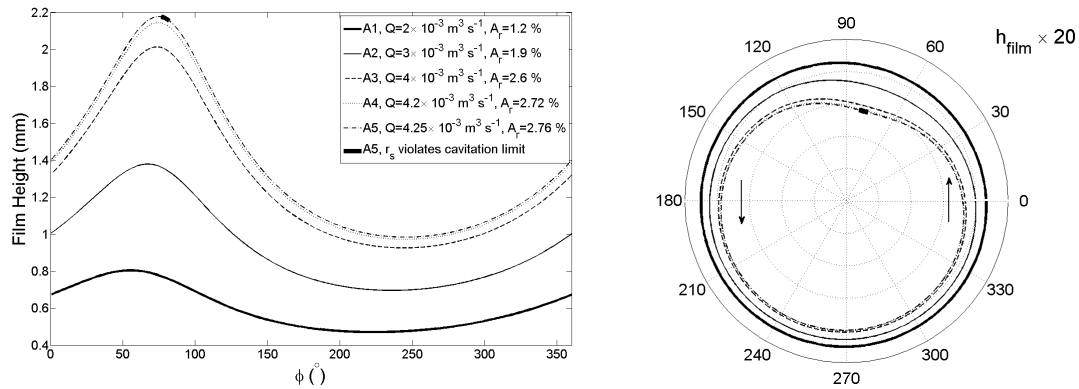


Figure 4: Results for cases A1 to A5

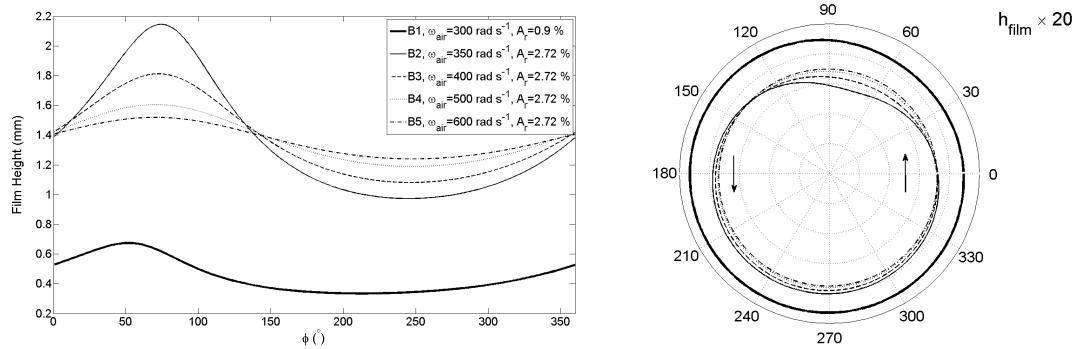


Figure 5: Results for cases B1 to B5

Table 4: Maximum fill fraction for various air speeds

$\omega_{air}$ (rad/s)	300	350	400
$A_{r,max}$ (%)	0.9	2.72	14.03

film was 0.9%. As can be seen from the figure and the data in Tab. 3, the increase in air speed causes an increase in film speed and a flattening of the film height profile. Interestingly at higher speed the peak in film thickness shifts towards the horizontal.

Lastly Tab. 4 summarizes maximum permissible fill fractions for a range of air speeds. If these fill fractions are exceeded, the cavitation criterion set by Eqn. 10 is violated and the film starts to detach. A strong dependence on air speed is observed. The data suggests that for the current geometry and shear force coefficients it is unlikely for a rimming film to exist at air speeds below 300rad/s (equivalent to  $30\text{ms}^{-1}$  at the gas-liquid interface).

### Conclusion

The development of a film model to predict the film thickness for a windage driven air film on the bore of a cylinder has been presented. In contrast to other film models, which are derived from lubrication theory, the current model incorporates the centrifugal acceleration term. The model is based on the assumption that a radially averaged velocity profile is present. This is an acceptable assumption as secondary recirculation vortices exist in the liquid, which facilitate a momentum exchange between the various liquid layers.

Model results for a range of test cases are presented, which show the formation of a peak in film height between the horizontal and vertical points on the side corresponding to liquid

upward flow. It was shown that increasing the quantity of liquid causes the amplitude of the peak to increase, until eventually the cavitation limit is violated at the film surface and the inner layers of the film start to fall radially inwards. Similarly it was shown that increasing the air speed, while maintaining the liquid level constant has a smoothing effect on the film.

### References

- [1] Benilov, E.S. and Benilov, M.S. and Kopteva, N., Steady rimming flows with surface tension, *Journal for Fluid Mechanics*, 597, 2008, pp91-118.
- [2] Chandra, B. and Simmons, K. and Pickering, S. and Tittel, M., Liquid and Gas Flow in Highly Rotating Environment, *ASME Conference Proceedings*, ASME, 2011, pp337-345.
- [3] Cohen, L.S. and Hanratty, T.J., Effect of waves at a gas-liquid interface on a turbulent air flow, *Journal of Fluid Mechanics*, 31, 1968, pp 467-479.
- [4] Gorse, P. and Busam, S. and Dullenkopf, K., Influence of operating Condition and Geometry on the Oil Film Thickness in Aeroengine Bearing Chambers, *Journal of Engineering for Gas Turbines and Power*, 128, January 2006, pp 103-110.
- [5] Villegas-Diaz, M. and Power, H. and Riley, D.S., Analytical and numerical studies of the stability of thin-film rimming flow subject to surface shear, *Journal of Fluid Mechanics*, 541, 2005, pp 317-344.
- [6] Whitham, G. B., *Linear and Nonlinear Waves*, JOHN WILEY & SONS, 1974.